Proceedings of CLIMA 2000 Conference; Congress Place, Brussels, Belgium; 8/30-9/ 2, 1997; Congress Place, Published on CDROM.

ON-LINE MONITORING AND FAULT DETECTION OF CONTROL SYSTEM PERFORMANCE

John E. Seem
Johnson Controls, Inc.
Milwaukee, WI 53211-0423
USA

John M. House
National Institute of Standards and Technology
Gaithersburg, MD 20899
USA

Richard H. Monroe
Johnson Controls, Inc.
Milwaukee, WI 53211-0423
USA

ABSTRACT

This paper presents a new method for monitoring the performance of control loops. The method determines performance indices using recursive relationships. The recursive formulation gives the method two desirable characteristics, namely, it is computationally efficient, and the memory requirements are small because only previous values of the performance indices are stored. Consequently, the method can be implemented in low-cost digital controllers, thereby reducing traffic on the communication network. Building operators can use the performance indices to quickly assess the performance of a large number of controllers. Performance indices may be used to quantify information about the amount of travel of an actuator, the difference between the desired process output and the actual output, saturation of a controller, etc. This paper presents laboratory and field test results demonstrating the utility of the performance indices for performance monitoring and fault detection in variable-air-volume air-handling units with pressure-independent variable-air-volume boxes.

INTRODUCTION

Modern control systems for heating, ventilating, and air-conditioning (HVAC) equipment contain a network of digital controllers connected on a communication trunk or bus. The digital controllers are used to control a wide variety of equipment such as boilers, chillers, air-handling units (AHU's), and variable-air-volume (VAV) boxes. There may be hundreds of digital controllers on a network for an HVAC control system. Control systems for large buildings frequently contain an operator workstation for monitoring system performance. In other control systems, the operator may monitor the system remotely by using modems to communicate with the digital controllers. Systems for small buildings, such as schools, may not be equipped with an operator workstation. In these systems, an operator may connect a portable computer or other commissioning device to the network to obtain information on system performance.

There are several different methods for connecting the digital controllers to the communication trunk. Hartman (1993) describes four different types of communication

networks that are used in the HVAC industry. Figure 1 depicts an architecture that uses peer-to-peer communications. In a peer-to-peer architecture, digital controllers, operator workstations, and modems all communicate on the same network.

Digital controllers and communication networks give building operators a vast capability to monitor the operation of HVAC systems. However, there are limitations to this capability. As with most computer systems, the limitations are memory requirements, computational speed, and network communication speed. While the workstation may have abundant memory and computational speed, network communication speed makes it difficult to sample all digital controllers at the same rate at which they are controlling (in many cases this can be every second). This problem is exacerbated in larger systems. Hence, whenever possible, computations that are performed on-line (i.e., at the same rate that the digital controller samples and controls a particular device) are shifted to the microprocessors within the digital controllers and information from the microprocessors is downloaded to the workstation much less frequently (every 15 minutes, hour, day, etc.). Today's microprocessors have limited computational resources, however, so it is not possible to execute complex, time consuming algorithms or store historical data at this level.

The objectives of this paper are to describe a control performance monitoring method that can alleviate the limitations associated with on-line monitoring of control system performance by compressing the data at the digital controller level, and to demonstrate the utility of the method for detecting faults in variable-air-volume (VAV) AHU's and boxes.

Descriptions of a typical VAV AHU and a typical pressure-independent VAV box and the control strategies utilized in these systems are presented first. Next, the control performance monitoring method is described. Laboratory and field test results demonstrating the use of the method for monitoring and detecting faults in VAV boxes and AHU's are then presented. Finally, conclusions of this study are presented.

SYSTEM DESCRIPTION

Figure 2 is a schematic diagram of a typical single duct VAV AHU. The primary function of an AHU is to provide conditioned air to various rooms. The AHU consists of variable speed supply and return fans, three dampers for controlling airflow to and from the AHU to the

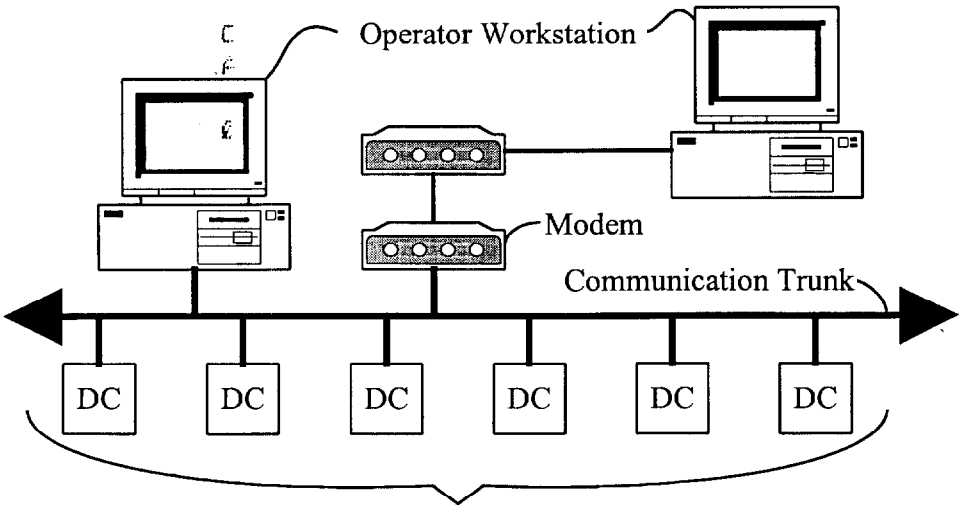

Figure 1 Communication architecture with peer-to-peer communications.

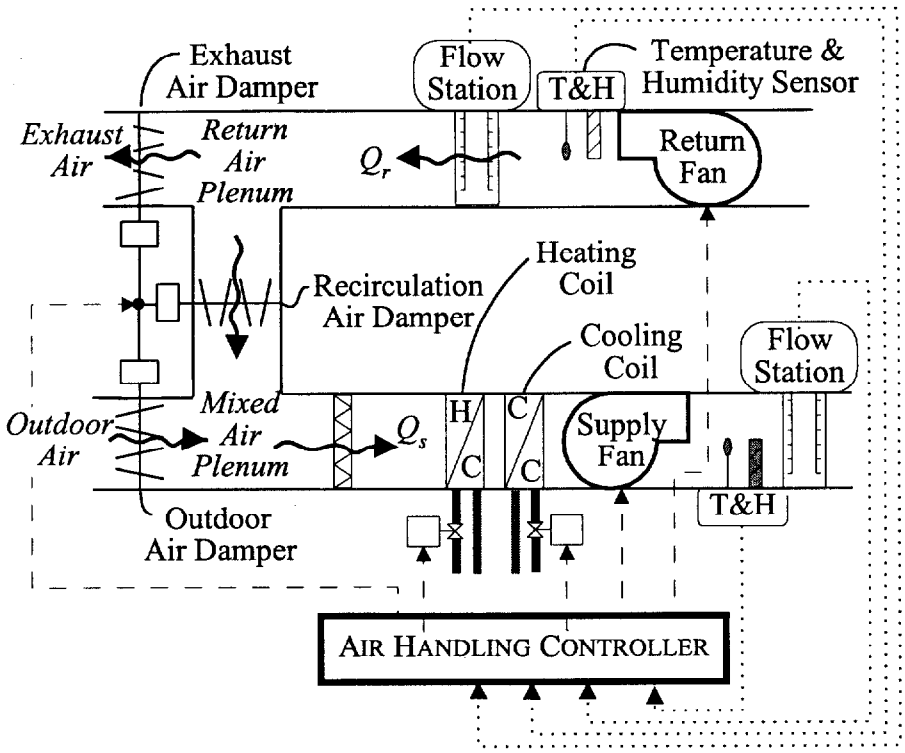

Figure 2 VAV AHU with a single duct.

outdoor environment, heating and cooling coils for conditioning the air, various sensors and actuators, and a controller that receives sensor measurements and computes and transmits new control signals. In the discussion that follows, normal operating strategies are described for a VAV AHU that uses volume matching control of the return fan.

VAV AHU's are typically controlled to maintain a constant setpoint temperature at some location in the supply duct downstream of the supply fan. This is achieved by controlling the outdoor air, recirculation air, and exhaust air damper positions, and by controlling the flow of hot water and cold water through the heating and cooling coils, respectively.

The supply fan of a VAV AHU is controlled to maintain the static pressure in the supply duct at a constant setpoint value. Constant temperature supply air is distributed to various zones (not shown), which may have different loads and setpoint temperatures. To account for the variability of the conditions in the zones, VAV boxes (not shown) that regulate the amount of air that enters a zone are placed at the end of the supply air ductwork leading to each zone. As a zone load decreases, the corresponding VAV box restricts the flow of air to the zone, thereby increasing the static pressure in the supply duct and causing the supply fan speed to decrease in order to maintain the static pressure setpoint condition. If the zone load increases, the VAV box and supply fan respond in the opposite manner.

There are several ways to control the return fan of a VAV AHU to maintain zone pressurization. With a volume matching control strategy, the return fan is controlled to maintain a constant differential between the supply and return airflow rates so that the zones have a small positive pressurization, thus reducing infiltration. Airflow stations are used to measure the airflow rates in the supply and return air ducts.

The control system for a pressure-independent VAV box is depicted in Figure 3. The pressure-independent VAV box has a damper for adjusting the flow rate of supply air into the room and a flow station for measuring the flow rate of air into the room. The thermostat is used to measure the room temperature, and some thermostats allow the building occupant to adjust the setpoint. Control systems for pressure-independent VAV boxes commonly use a

cascade control strategy to maintain the zone temperature at the setpoint value. The cascade control strategy is shown in Figure 4. The temperature controller determines the setpoint for the flow controller. The secondary control loop for flow is nested inside the temperature control loop.

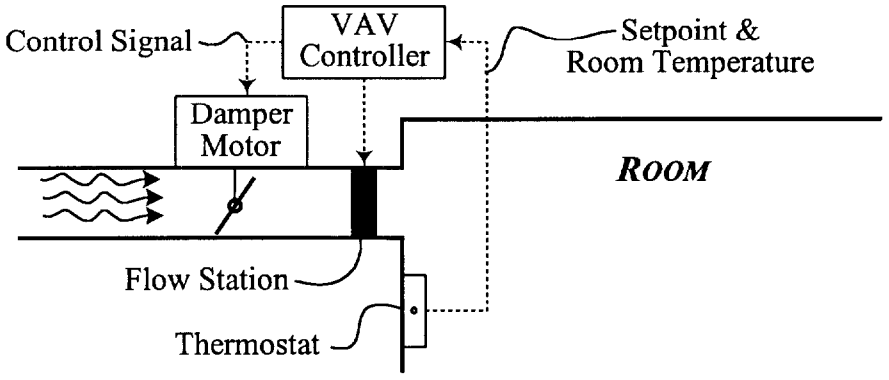

Figure 3 Control system for pressure-independent VAV box.

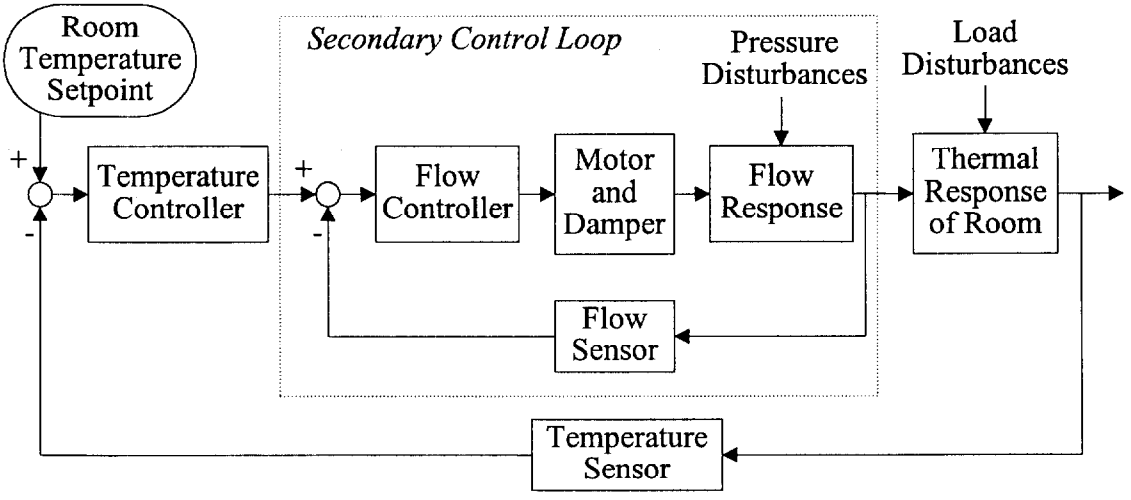

Figure 4 Block diagram for cascade control of room temperature implemented in pressure-independent VAV box controllers.

CONTROL PERFORMANCE MONITOR

The control performance monitoring algorithm is used to compute indices that quantify control system performance. Examples of performance indices are the duty cycle of a motor and the number of starts, stops, and reversals of an actuator. Both of these indices are useful for identifying unstable control that can lead to excessive component wear. Figure 5 is a block diagram of a digital control system that has a control performance monitor. The feedback controller adjusts the actuator to bring the sensed value for the process output toward the setpoint. Simultaneously, the control performance monitor collects data (i.e., error signal to

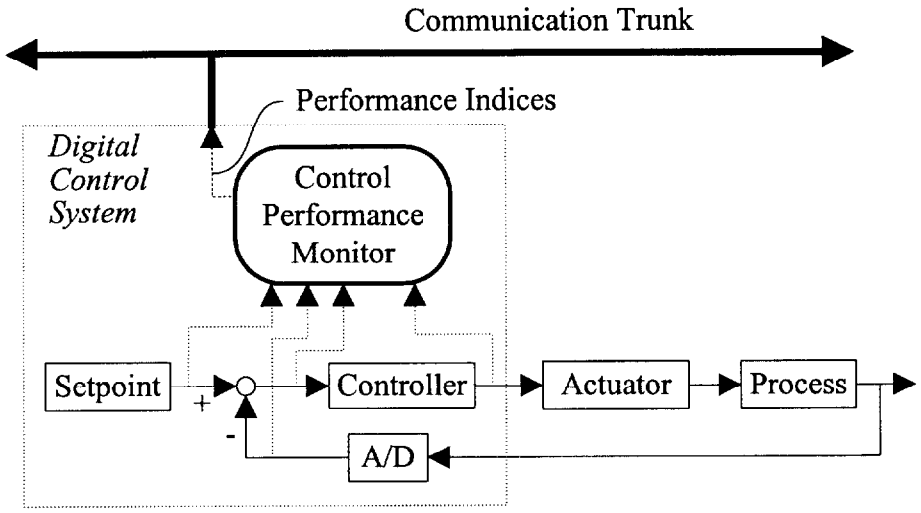

Figure 5 Single loop feedback control system with control performance monitor.

the controller, change in the control signal, and process output) and computes indices that quantify the controller performance. The control performance monitor determines estimates of the indices using exponentially weighted moving averages (EWMA's).

The equation for computing an EWMA is given by (Hunter, 1986)

$$\bar{X}_t = \sum_{j=0}^{\infty} \lambda (1 - \lambda)^j X_{t-jT} \tag{1}$$

where

$\bar{X}_t$	=	EWMA of performance index X at time t
λ	=	exponential smoothing constant
X_{t-jT}	=	value of performance index X at discrete time $t - jT$
T	=	sample time for analog-to-digital converter

Pandit and Wu (1983) refer to the term $\lambda (1 - \lambda)^j$ as an exponential smoothing weight. Equation 1 is called an exponentially weighted moving average because the exponential smoothing weights decrease exponentially or geometrically as j increases (Box and Jenkins, 1976). Figure 6 shows the relationship between the exponential smoothing weights and j for λ equal to 0.2 and 0.5. As λ increases, the weights decrease at a faster rate. Consequently, more past data will affect the EWMA when λ is small. Montgomery (1991) describes the use of EWMA control charts and claims that values of λ between 0.05 and 0.25 work well in practice. Pandit and Wu (1983) recommend that the value of λ should be between 0 and 0.3.

To implement Equation 1 in computer code, it would be necessary that all past data be stored in computer memory. However, Equation 1 can be reformulated as

$$\bar{X}_t = \bar{X}_{t-T} + \lambda \left(X_t - \bar{X}_{t-T} \right) \tag{2}$$

Equation 2 is a recursive form of Equation 1. An important advantage of Equation 2 is that only the previous value of the smoothed estimate of the performance index must be stored. By comparison, if a typical moving average (Seborg et al., 1989) is to be computed, all past values of the variable being averaged must be stored in memory. If moving averages are

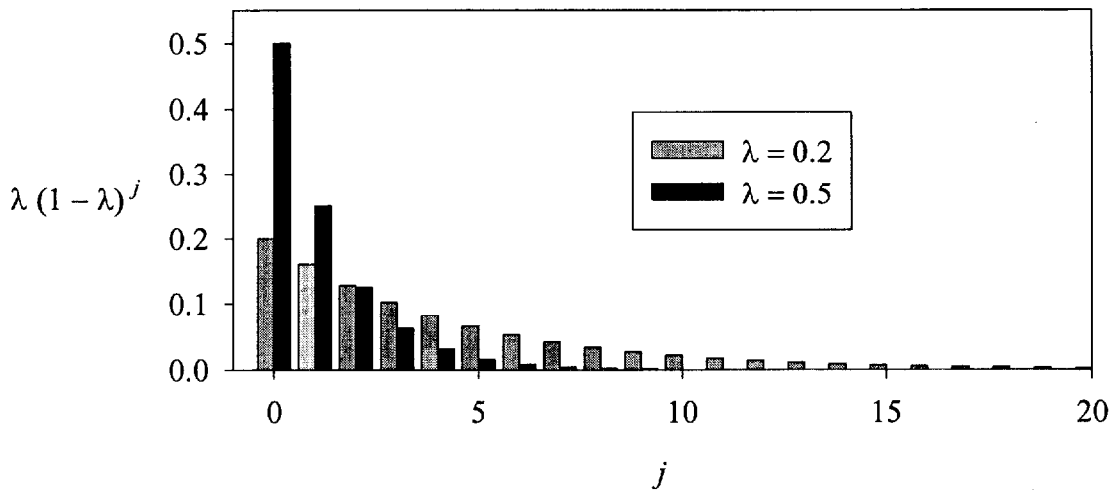

Figure 6 Exponential smoothing weights for smoothing constants of 0.2 and 0.5.

desired for numerous variables, there may be insufficient memory to store the necessary data.

Equation 2 should only be used during time periods that the controller is operating. Also, a building controls engineer may want to use Equation 2 only during occupied time periods. Some controllers have built in diagnostics for confirming that a sensor is connected to the controller. If a controller detects that a sensor is not connected, then the controller can issue a command that a sensor failure has occurred. The EWMA should not be updated during time periods that the controller has detected a sensor failure.

When monitoring the performance of a feedback control system with an EWMA, the smoothing constant, λ, needs to be chosen carefully. If the smoothing constant is too large (e.g., if $\lambda = 1$, the EWMA is equal to the current point measurement), the EWMA will take on large values following a load disturbance or setpoint change. This may cause the performance monitor to indicate a fault when no fault is present. If the smoothing constant is too small, it will take a long time for the performance monitor to detect a fault. The following guidelines can be used to select a smoothing constant based on the response characteristics for a feedback control system::

$$\frac{T}{20\,t_s} < \lambda < \frac{T}{5\,t_s} \tag{3}$$

where

T = sampling time of the analog-to-digital converter
t_s = settling time of the controller

When $\lambda = T/5t_s$, the summation of the exponential smoothing weights between times t and $t - 5t_s$ is approximately 0.632. This means that approximately 63.2% of the EWMA is based on the data between times t and $t - 5t_s$. When $\lambda = T/20t_s$, approximately 63.2% of the EWMA is based on the data between times t and $t - 20t_s$.

Figure 7 shows a typical closed-loop response to a step change in setpoint and the settling time. The settling time is the time required for the process output to settle to and remain within $\pm\ \delta$ of the final value. Common values for δ are 1%, 2%, or 5% of the size of the setpoint change (Åström and Hägglund, 1995, and Seborg et al., 1989).

Performance indices computed using EWMA's make it practical to simultaneously

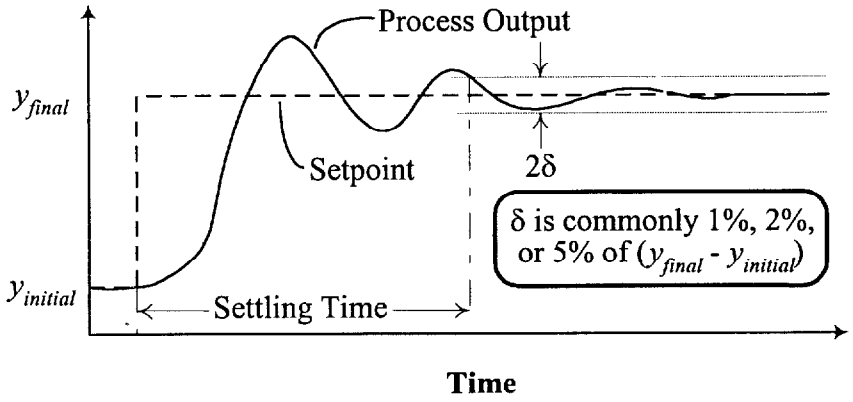

Figure 7 Settling time specification for step change in setpoint.

monitor the recent performance of hundreds of local digital controllers because they effectively compress the performance data. Because the EWMA algorithm is numerically efficient and requires very little memory, it can be used in today's digital control systems to compute performance indices on-line. There are several possible uses of the performance indices:

1) The performance indices can be used to compare the performance of similar controllers. For instance, a building operator can download performance indices for a large number of VAV boxes from the digital controllers to a central workstation and quickly compare the performance of the controllers. Because of the similarity of the controllers and the controlled devices, controllers demonstrating poor performance can be readily identified. The operator can then collect additional data and/or assign a service person to inspect the controller and HVAC system.

2) The performance indices can be used in a real-time fault detection system to determine a fault in a control system or component of the HVAC system. A fault is determined by comparing the performance indices with control limits that are determined either by expert knowledge of the system or by using methods from statistical quality control (Montgomery, 1991).

3) A diagnostic system can be developed that uses patterns of performance indices to identify possible causes of a fault.

There are a number of performance indices that could be used to assess control system performance. Seven performance indices are listed in Table 1. The EWMA of the process error e is a good performance index for comparison of different control systems or algorithms. The process error is the difference between the desired process output y_{set} and the actual process output y. The EWMA of the absolute value of the process error $|e|$ is an even better performance index for this purpose because positive and negative errors associated with unstable control do not cancel one another. The EWMA of the process output y gives information similar to that of the EWMA of the process error, although the index for the process output may be more illustrative in some circumstances. Controller stability and the amount that an actuator is driven can be assessed using the EWMA for the absolute value of the change in the control signal $|\Delta u|$. The EWMA of the control signal u is useful for determining when a controller is saturated. Like $|\Delta u|$, the EWMA of the duty cycle of an electric motor d and the EWMA of the number starts, stops, and reversals of an actuator S can

Table 1 Performance indices for monitoring control system operation.

Performance Index Description	Mathematical Expression
process error, e[1]	$\bar{e}_t = \bar{e}_{t-T} + \lambda\left(e_t - \bar{e}_{t-T}\right)$
absolute value of process error	$\lvert \bar{e}_t \rvert = \lvert \bar{e}_{t-T} \rvert + \lambda\left(\lvert e_t \rvert - \lvert \bar{e}_{t-T} \rvert\right)$
process output, y	$\bar{y}_t = \bar{y}_{t-T} + \lambda\left(y_t - \bar{y}_{t-T}\right)$
absolute value of change in control input, Δu	$\lvert \overline{\Delta u_t} \rvert = \lvert \overline{\Delta u_{t-T}} \rvert + \lambda\left(\lvert \Delta u_t \rvert - \lvert \overline{\Delta u_{t-T}} \rvert\right)$
control input, u	$\bar{u}_t = \bar{u}_{t-T} + \lambda\left(u_t - \bar{u}_{t-T}\right)$
duty cycle, d	$\bar{d}_t = \bar{d}_{t-T} + \lambda\left(d_t - \bar{d}_{t-T}\right)$
number of starts, stops, and reversals, S	$\bar{S}_t = \bar{S}_{t-T} + \lambda\left(S_t - \bar{S}_{t-T}\right)$

[1] $e = (y_{set} - y)$

be related to controller stability and actuator wear. As mentioned previously, most if not all of the performance indices can be used in a straightforward manner to detect faulty operating conditions.

EWMA's of the performance indices can be computed in the operator workstation using signals from the digital controllers. However, there are several advantages to determining the EWMA's in the digital controllers. Two of these advantages have been alluded to previously, namely, that communication rates on the network would be improved because the frequency at which data needs to be transferred on the network is reduced, and that the amount of processing that needs to be performed in the operator workstation would be reduced. A third advantage of computing the performance indices in the digital controllers is that a system representative could connect a portable computer to the network and read the performance indices for various controllers. This would be important for control systems that did not have an operator workstation on the communication trunk. Finally, there are times when the communication network is not connected or is malfunctioning. After the network communication is re-established, a building operator could quickly determine the performance of the control system by pulling down data from the local digital controllers.

Control Performance Monitoring of Laboratory VAV Boxes

Control systems for VAV boxes have a number of components that may fail. For example, the damper could stick, the damper motor could fail, there could be a problem with the flow station, or the airflow controller could be unstable. To demonstrate the use of performance indices to monitor the operation of VAV boxes, two faults are introduced in a laboratory AHU that is equipped with three pressure-independent VAV boxes. The laboratory VAV boxes use electrical controls, thus, the performance indices are computed at the central workstation. This negates the benefit of reduced network traffic that results from implementing the indices in local digital controllers, but makes it possible to demonstrate the utility of the performance indices.

A block diagram depicting the control system for the laboratory VAV boxes and the implementation of the performance indices to monitor the boxes is shown in Figure 8. This control system is slightly different from the block diagram representation in Figure 4. The VAV boxes do not control the temperature in individual zones; they deliver the supply air to a common zone. Thus, rather than using room thermostat signals and the temperature controller

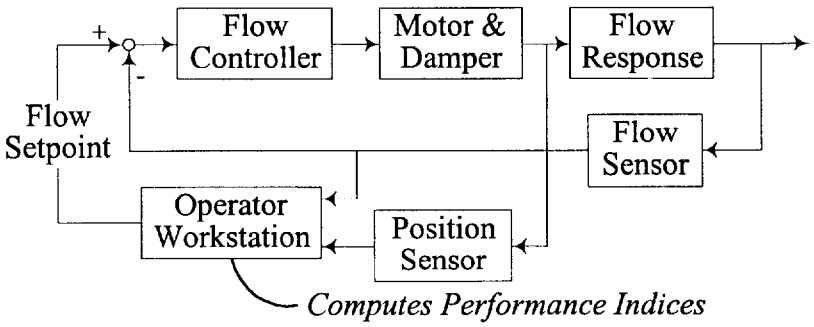

Figure 8 Block diagram representing the implementation of airflow error and damper position performance indices in pressure-independent VAV boxes in a laboratory AHU.

to adjust the setpoint to the flow controller, this setpoint is established artificially by sending a voltage signal from the operator workstation (via a data acquisition and control unit) to the individual VAV boxes. In addition, the laboratory VAV boxes are each equipped with a potentiometer for measuring the damper position. This does not affect the control of the VAV boxes; however, damper position will be used to monitor the operation of the VAV boxes.

The first fault considered was a stuck damper in a VAV box. This fault causes the error signal to the airflow controller to increase as the zone load changes. The zone load profile for the occupied period of the day is represented by the setpoint voltage signal sent to the VAV boxes. The setpoint voltage signal is shown in Figure 9a. The same signal is sent to all VAV boxes for the initial two and one-half hours of the test, however, the signal sent to VAV box 3 is then held constant over the remainder of the test to simulate a stuck damper fault.

For this fault, the operation of the VAV boxes was monitored using a performance index for the airflow error of each box. The absolute airflow error performance index is given by

$$| \bar{e}_t | = | \bar{e}_{t-T} | + \lambda \left(| e_t | - | \bar{e}_{t-T} | \right) \tag{4}$$

where

$| e_t | = \left| Q_{set} - Q_t \right|$ is the absolute value of the difference in the setpoint and actual airflow rates at time t

$| \bar{e}_t |$ = EWMA of absolute airflow error at time t

The sampling time for controlling the VAV boxes was 1.5 seconds, hence, $| \bar{e}_t |$ was updated every 1.5 seconds. The smoothing constant was set to 0.002. The normalized absolute airflow error performance index for each of the three VAV boxes is shown in Figure 9b at fifteen minute intervals for eight hours of a nine hour test period. The initial hour is not presented because the results are overly influenced by startup transients that are much more severe than normal load or setpoint changes. Normalized values were obtained by dividing the airflow errors by the maximum setpoint airflow rate for the test. The existence of a fault in VAV box 3 is evident from Figure 9b.

The second fault is an unstable supply air pressure controller. Because the airflow controllers in the pressure-independent VAV boxes attempt to maintain the airflow rates at the setpoint values, this fault can lead to the constant adjustment of the damper positions and therefore, excessive wear of the actuators. To implement this fault, the proportional gain for the proportional plus integral controller that controls the supply fan was increased by a factor

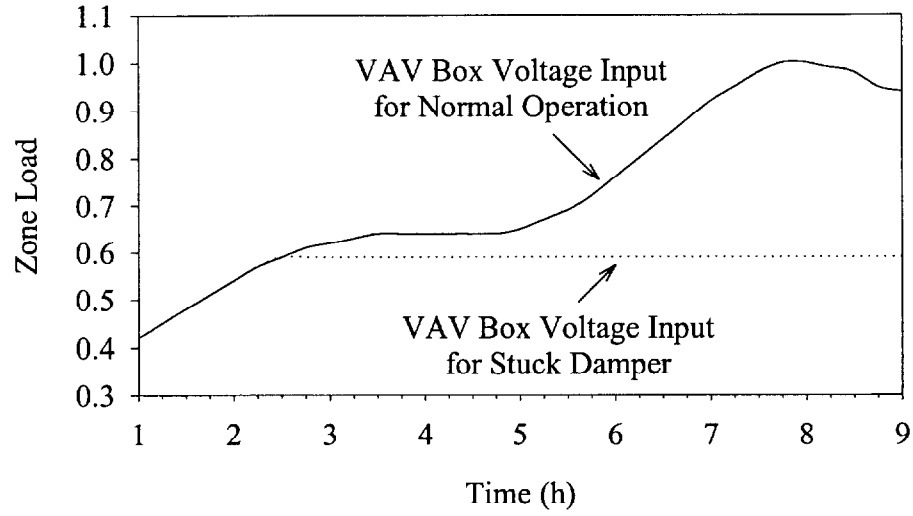

Figure 9a Voltage inputs to the VAV box flow controllers.

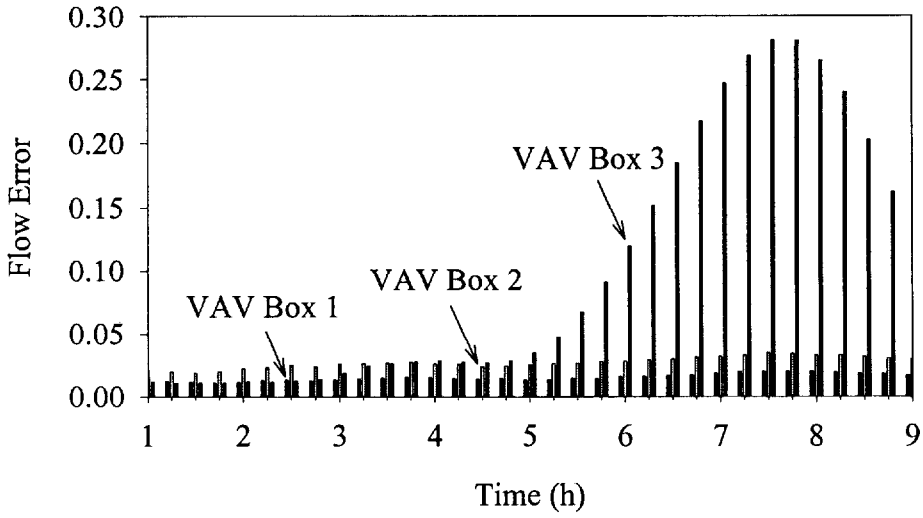

Figure 9b Voltage inputs to the VAV box flow controllers.

of 4.5 after two and one-half hours of operation, and the supply pressure setpoint was increased from 249 to 274 Pa after four hours of operation. To isolate the effect of the unstable supply pressure from other effects that would tend to make the VAV box dampers open and close, a constant setpoint voltage was sent to the three VAV boxes, thereby simulating constant loads for each zone. The movement of the VAV box dampers is quantified using an EWMA of the absolute value of the change in the potentiometer signal for each damper.

The supply air pressure is plotted in Figure 10a for a six hour period and the corresponding EWMA's for the absolute airflow error and the absolute value of the change in position (indicated by a change in voltage from a potentiometer) of each VAV box damper are plotted in Figures 10b and 10c. A smoothing constant of 0.002 was used for these results. Figure 10a shows that the supply air pressure begins to oscillate shortly after the change in the proportional gain at $t = 2.5$ h, where t denotes time. The oscillations are less severe just prior to the setpoint change; however, after the change there were sustained oscillations with a peak to peak amplitude of approximately 120 Pa. Figures 10b and 10c show that the

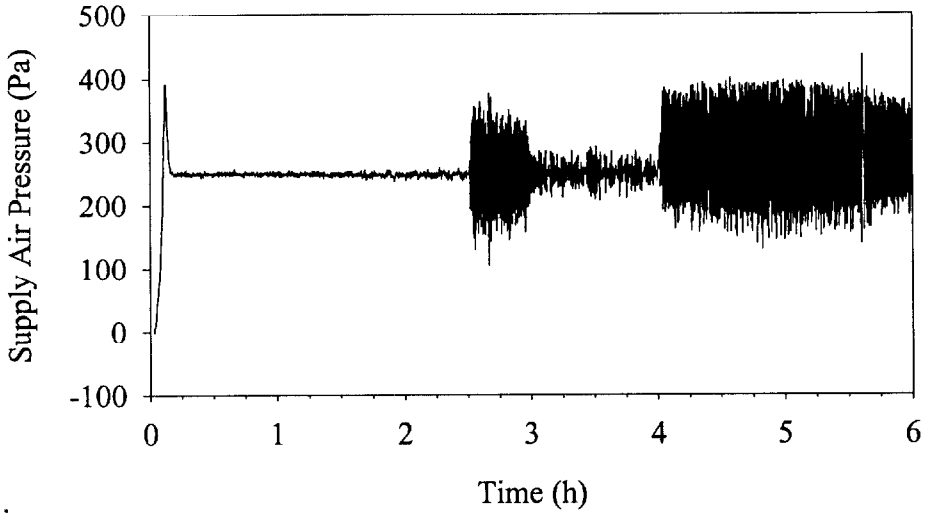

Figure 10a Unstable supply air pressure response.

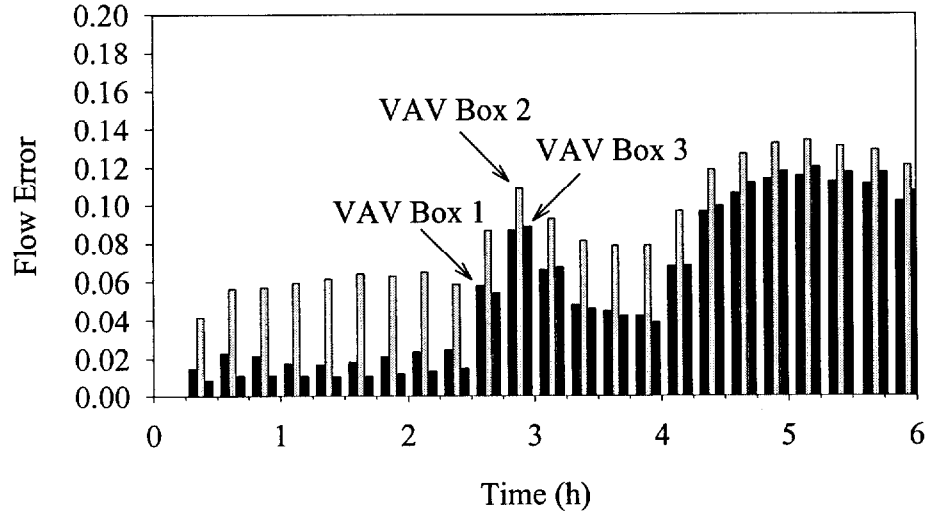

Figure 10b Normalized absolute airflow error for the three VAV boxes.

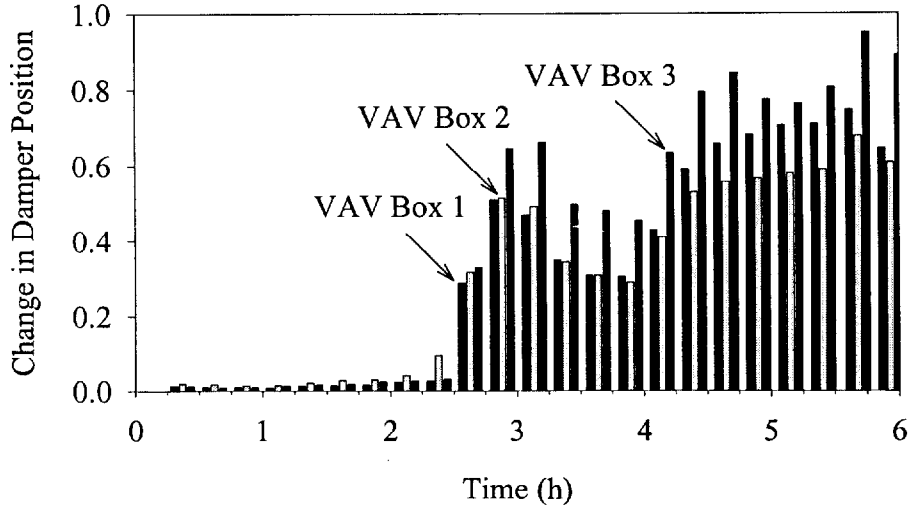

Figure 10c Normalized absolute change in damper position for the three VAV boxes.

instability of the supply air pressure is manifested in continuous movement of the dampers in the VAV boxes. The larger the amplitude of the oscillations of the supply air pressure, the greater the value of the EWMA's for both the absolute airflow error and the absolute change in the VAV box damper position. As the oscillations are suppressed, the EWMA's also decrease. For this case, the change in damper position is a more reliable indication of the presence of a fault than the absolute airflow error. However, for the stuck damper fault, the opposite would be true.

The results in Figure 10 demonstrate a straightforward method of detecting an unstable supply air pressure controller. For VAV boxes with digital controllers, the absolute value of the change in the control signal to the damper actuator could be used instead of the potentiometer voltage to detect this fault, as well as unstable VAV box flow controller faults.

Control Performance Monitoring of a Laboratory VAV AHU

Lee et al. (1996a, 1996b) studied the symptoms of eight complete faults for a VAV AHU and trained an artificial neural network (ANN) to identify an idealized pattern of the symptoms for each fault. In this study, EWMA's for the control signal u, the absolute value of the change in the control signal Δu, the process error e, and the absolute value of the process error $|e|$ for the supply fan, return fan, and cooling coil valve control loops were used to examine six of the faults considered by Lee et al. (1996a, 1996b). Control loops for the heating coil valve and mixing box dampers were not considered. The six faults examined were as follows:

- Complete failure of the supply fan
- Complete failure of the return fan
- Stuck cooling coil valve
- Complete failure of the supply air thermocouple
- Complete failure of the supply air flow station
- Complete failure of the return air flow station

Unless noted otherwise, faults were introduced three hours after the commencement of a test and operation continued for two hours after the occurrence of a fault. With the exception of the supply air thermocouple fault, all faults were introduced by disconnecting or turning off the power to sensors or actuators. The supply air thermocouple fault was introduced through software changes. In the results that follow, only EWMA's are presented. Time series responses of the actual control signal, process error and related variables are not presented. The EWMA's respond at a much slower rate than the actual variables that are used by the controllers. For all results presented in this section, the smoothing constant for the cooling coil valve controller, supply fan controller, and return fan controller are 0.000333, 0.005, and 0.0025, respectively.

Figure 11 shows the evolution of the performance indices for a complete failure of the supply fan. During normal operation the supply fan was controlled to maintain a static pressure of 249 Pa in the supply air duct and the return fan was controlled to maintain a flow difference of 0.472 m^3/s between the supply and return air ducts. The fault caused the supply fan rotational speed to decrease to zero. Figure 11a shows the performance indices for the cooling coil valve controller. Because there was no air flow, the supply air temperature gradually increased, as evidenced by the decrease in $\bar{e}$. Two hours after the occurrence of the fault, the EWMA of the cooling coil valve process error was approximately -2°C. The rise in the supply air temperature caused the cooling coil valve control signal to increase to its maximum value, although $\bar{u}$ did not saturate in the time allotted for this test. If the test length was extended, $\bar{u}$ would eventually saturate. The absolute value of the change in the control

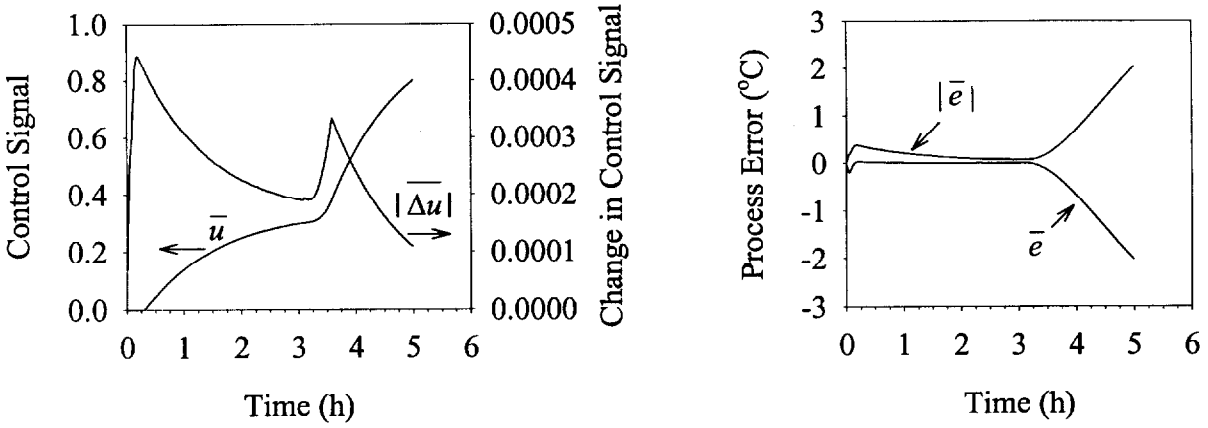

Figure 11a Cooling coil valve performance indices for a complete supply fan failure.

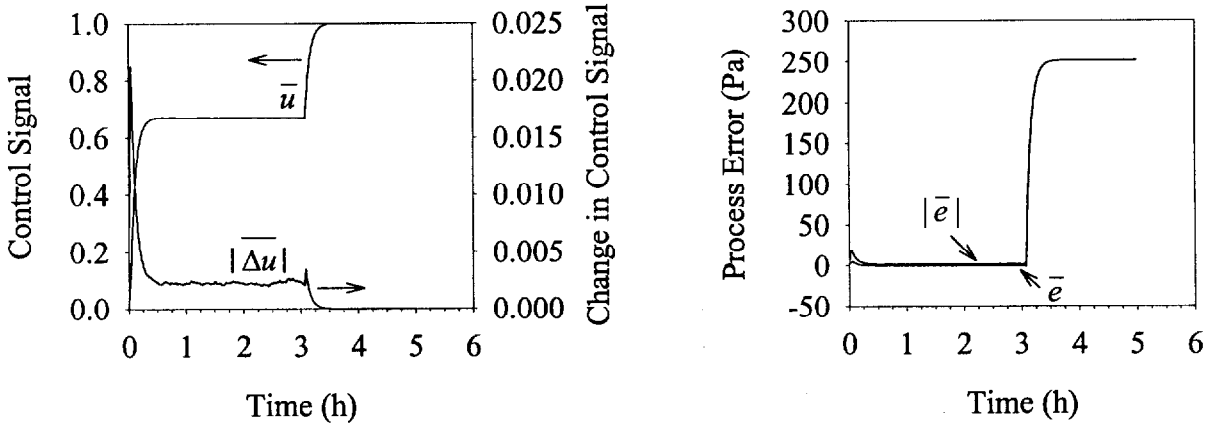

Figure 11b Supply fan performance indices for a complete supply fan failure.

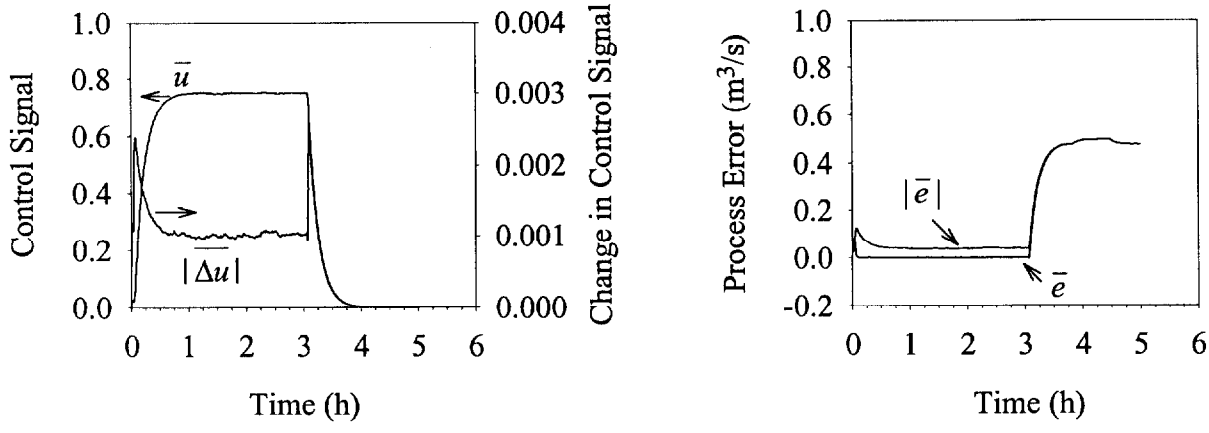

Figure 11c Return fan performance indices for a complete supply fan failure.

signal $|\Delta u|$ initially increased rapidly after the fault occurred; however, once the controller saturated, $|\Delta u|$ decayed toward zero. This type of response was also seen for $|\Delta u|$ for the other control loops. Figure 11b shows the performance indices for the supply fan controller for the supply fan fault. The fault caused the supply air pressure to decrease to zero. This yielded values of $\bar{e}$ and $|\bar{e}|$ equal to 249 Pa for the supply fan controller. As evidenced by the response of $\bar{u}$, the fault also caused the control signal to the supply fan to increase to its

maximum value in an attempt to offset the decreasing supply air pressure. The performance indices for the return fan controller are shown in Figure 11c. Because there is no air flow in the supply duct, the return fan controller quickly shut down the return fan in an attempt to maintain the flow difference between the supply and return air ducts at the setpoint value. The fault caused $\bar{e}$ for the return fan controller to approach the process setpoint value of 0.472 m^3/s, while $\bar{u}$ saturated at its minimum value.

Plots of the return fan controller performance indices for a complete failure of the return fan are shown in Figure 12. For this and the remaining faults, only the performance indices for the controllers that are significantly affected by a given fault are presented. The fault caused the return fan rotational speed to decrease to zero. This caused the flow difference between the supply and return ducts to increase, which yielded a large negative value of $\bar{e}$. In addition, the negative error caused the control signal to the return fan to increase to its maximum value, thus causing $\bar{u}$ to saturate at its maximum value. After increasing rapidly after the occurrence of the fault, $|\Delta u|$ decayed to zero once u saturated.

Plots of the cooling coil valve controller performance indices for stuck cooling coil valve are shown in Figure 13. The fault was introduced three hours into the test, and near normal operation continued until a zone load increase was imposed on the three VAV boxes at $t = 4$ h. The load increase caused the damper of each VAV box to open, thus decreasing the static

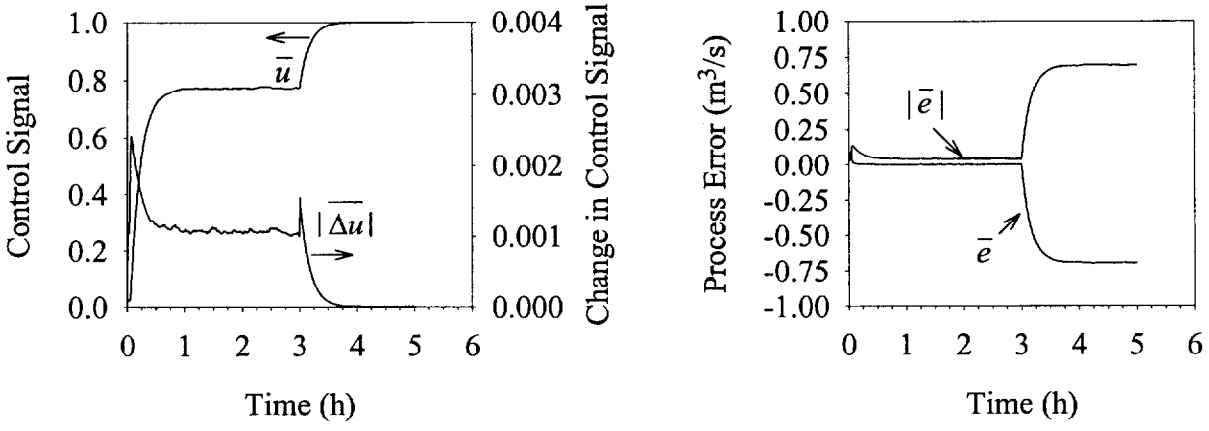

Figure 12 Return fan performance indices for a complete return fan failure.

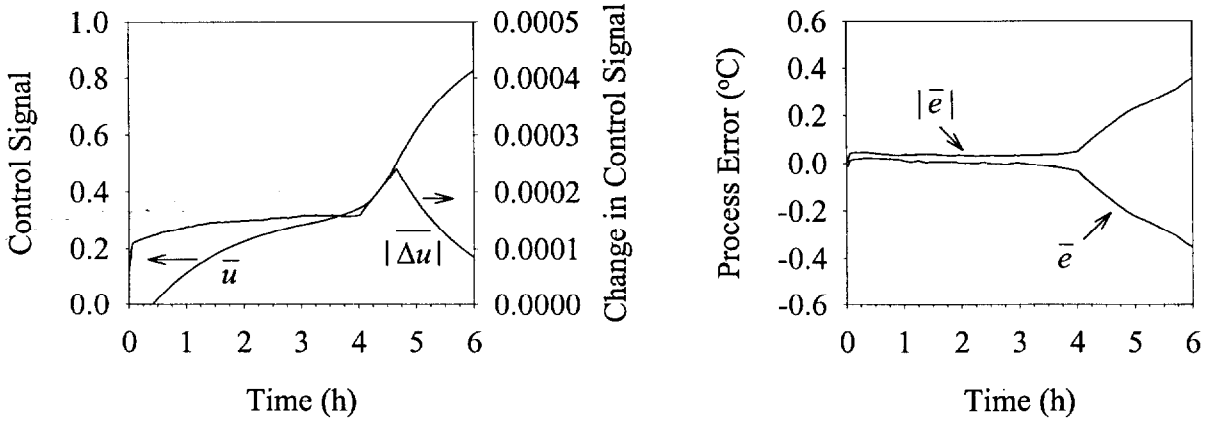

Figure 13 Cooling coil valve performance indices for a stuck cooling coil valve.

pressure in the supply duct. This caused the supply fan speed to increase to bring the static pressure back up to the setpoint value and, consequently, the supply air temperature increased. The resultant effect of the fault is that $\bar{e}$ is approximately equal to -0.4°C at the end of the test. In an attempt to compensate for the increasing supply air temperature, the control signalto the cooling coil valve increased toward its maximum value and eventually saturated, and approached unity. Given additional time, $\bar{u}$ would also saturate and would remain saturated until a significant load decreasc occurred. In addition, the fault caused a rather obvious change in the value of $|\Delta u|$. At first $|\Delta u|$ increased as the control signal increased. However, once the control signal saturated, $|\Delta u|$ began to decrease toward zero.

Performance indices for the cooling coil valve controller are plotted in Figure 14 for a supply air thermocouple failure. A complete thermocouple failure typically results in a voltage signal that varies randomly between large positive and large negative values. If the sensed value of the supply air temperature is outside of the range of normal operating conditions (0 to 40°C, for example), the temperature could be automatically set to zero so that the temperature would not fluctuate. This failure was simulated by overwriting the measured supply air temperature with a value of 0°C. This caused $\bar{e}$ and $|\bar{e}|$ to increase and approach the supply air setpoint value of 14.5°C, while $\bar{u}$ decreased to its minimum value. Because of the abrupt change in the supply air temperature caused by setting it equal to 0°C, $|\Delta u|$ increased very rapidly and then began to decay toward zero since u was saturated at its minimum value.

Return fan performance indices are plotted in Figure 15 for a complete failure of the supply fan flow station. This fault caused the return fan to shut down because the supply flow station indicated that there was no flow in the supply duct. Thus, the control signal u to the return fan decreased to its minimum value in an attempt to maintain the flow difference between the supply and return ducts at the setpoint value. The process errors $\bar{e}$ and $|\bar{e}|$ were approximately equal to 0.37 m^3/s at the conclusion of the test, while $\bar{u}$ decayed to zero. As in all cases where a controller saturated, $|\Delta u|$ also decayed to zero after a rapid increase immediately following the fault.

Return fan controller performance indices are plotted in Figure 16 for a complete failure of the return fan flow station. When this fault occurred, a zero reading was obtained for the return flow station. Thus, the control signal u to the return fan increased to its maximum value in an attempt to maintain the flow difference between the supply and return ducts at the setpoint value. The response of the performance indices for the return fan controller for this fault are almost identical to those observed for the return fan failure.

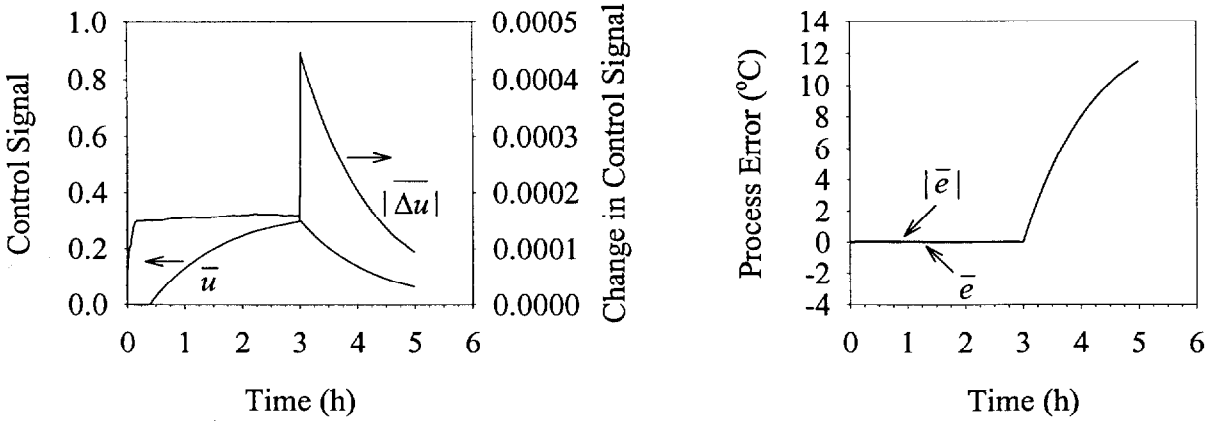

Figure 14 Cooling coil valve performance indices for a supply air thermocouple fault.

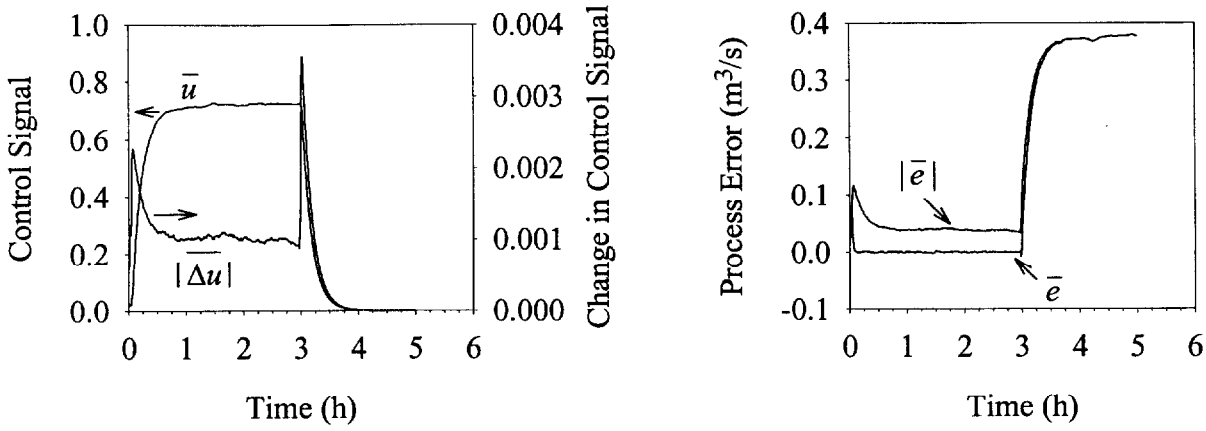

Figure 15 Return fan performance indices for a complete supply flow station failure.

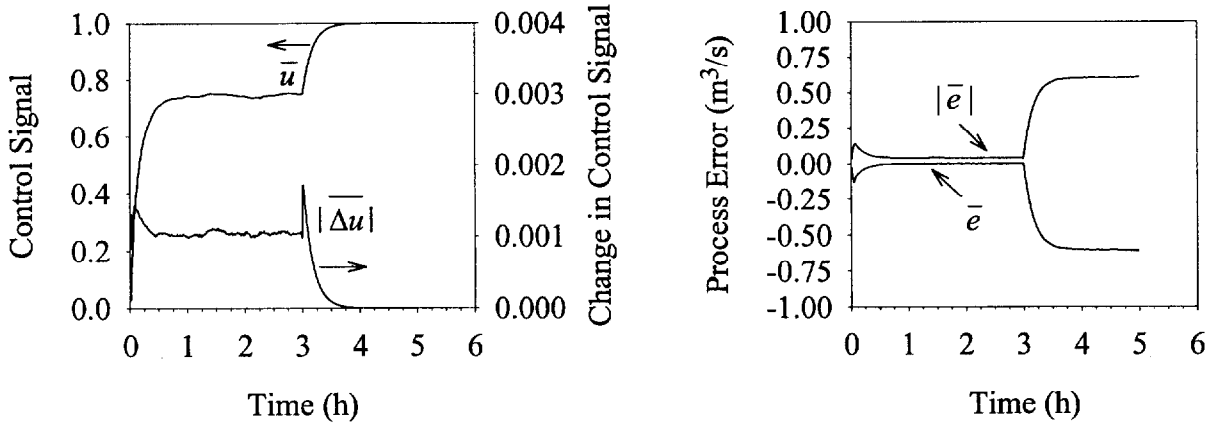

Figure 16 Return fan performance indices for a complete return flow station failure.

Control Performance Monitoring of Real Building VAV Boxes

The true value of the performance indices is better understood if one considers the task of simultaneously monitoring tens or hundreds of VAV boxes. For that scale of a system, the performance indices must be computed in the individual digital controllers and plots such as Figure 9b present only the current values of the performance indices for each of the VAV boxes. This technology exists today in real buildings. Currently, over 100,000 digital VAV controllers have the capability of determining the following three performance indices: duty cycle, EWMA of absolute value of the flow error, and EWMA of the absolute value of the temperature error. The VAV controllers are commissioned by a building operator, who responds to queries from commissioning software to select the performance indices to be computed.

In one particular building, a subcontractor installed new digital controllers for 24 dual-duct VAV boxes (Wang, 1993) that were located on the 21st floor of a 28 story office building. The digital controllers sampled the controlled variables every 1.5 seconds. The smoothing constant for the flow error was 0.000833 and the smoothing constant for the temperature error was 0.000104. An average duty cycle was determined from the last time the controller was reset. The subcontractor and building engineer were confident that the VAV controllers were correctly installed and operating properly.

Figure 17a shows the normalized flow error for the 24 VAV boxes. The flow errors were normalized by dividing the EWMA of the absolute value of the flow error by the design maximum flow rate for cooling. The normalized flow errors for boxes 16 and 18 are significantly larger than the flow errors for the other boxes. After further investigation, the building engineer determined that the electric motor for box 16 had a defective capacitor. Also, it was determined that the electric actuator for box 18 was incorrectly installed. Specifically, the electric damper actuator had been locked to the damper shaft 90 degrees from the correct position. This caused the VAV box to be wide open when the VAV controller issued a closed command, and to be completely closed when the VAV controller issued a command for full flow. A detailed description of the VAV box damper actuator installation is provided in the Appendix.

For the fault free VAV boxes (i.e., boxes 1 to 15, 17, and 19 to 24), the average normalized flow error was 0.047 and the standard deviation was 0.027. For VAV boxes 16 and 18, the normalized flow errors were 0.866 and 1.136, respectively. These flow errors are 30 and 40 standard deviations larger than the average value for fault free boxes.

Figure 17b shows the duty cycle for the 24 VAV boxes. There appears to be no significant outlier in the duty cycle for the VAV boxes. If a control system for one of the VAV boxes was unstable, a high duty cycle and a large normalized flow error would be expected for that particular box.

Figure 17c shows the EWMA of the absolute value of the temperature errors for the 24 VAV controllers. Notice that although four boxes have temperature errors above 1°C, the errors are not deemed to be significant enough by themselves to warrant further attention from the building operator. Figure 17d is a plot of the EWMA of the temperature errors versus the EWMA of the normalized flow errors. Both boxes 16 and 18 have large flow errors. This figure can help a building operator prioritize maintenance for boxes with the high normalized flow errors by establishing which of the boxes has the highest temperature error and therefore, the highest likelihood of uncomfortable occupants. Although box 18 has a larger flow error than box 16, box 16 should probably be examined and fixed first because of the large temperature error associated with this box.

CONCLUSIONS

This paper presented a new method for monitoring the performance of control loops. The method determines performance indices using recursive relationships. This makes the method computationally efficient, and minimizes the computer memory requirements because only previous values of the performance indices are stored. Consequently, the method can be implemented in low-cost digital controllers, thus reducing network traffic caused by monitoring variables at the central workstation. Building operators can use the performance indices to quickly assess the performance of a large number of controllers.

This paper presented laboratory and field test results demonstrating the utility of the performance indices for performance monitoring and fault detection in variable-air-volume air-handling units with pressure-independent variable-air-volume boxes. Fault detection could be further automated by combining the performance monitoring method with thresholds obtained through expert knowledge or by application of the principles of statistical quality control.

ACKNOWLEDGMENTS

This research was partially supported by the Office of Energy Efficiency and Renewable Energy, U. S. Department of Energy.

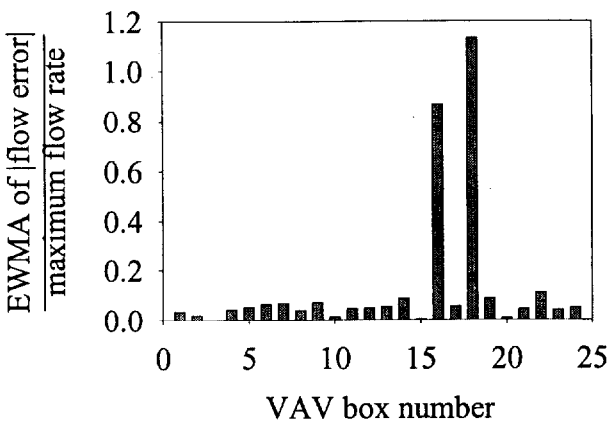

Figure 17a Normalized flow errors.

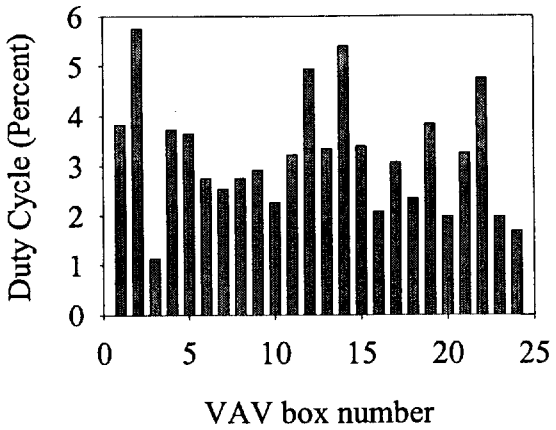

Figure 17b Duty cycle.

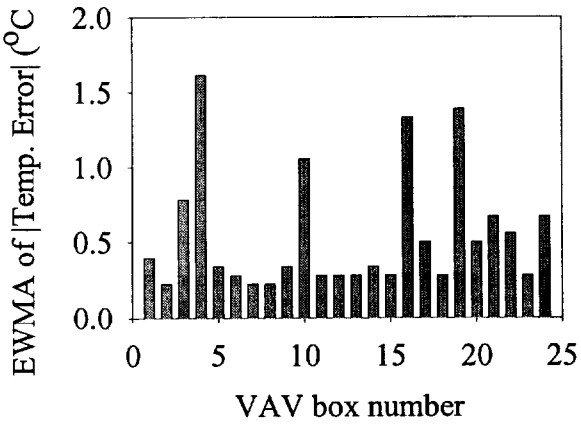

Figure 17c Temperature errors.

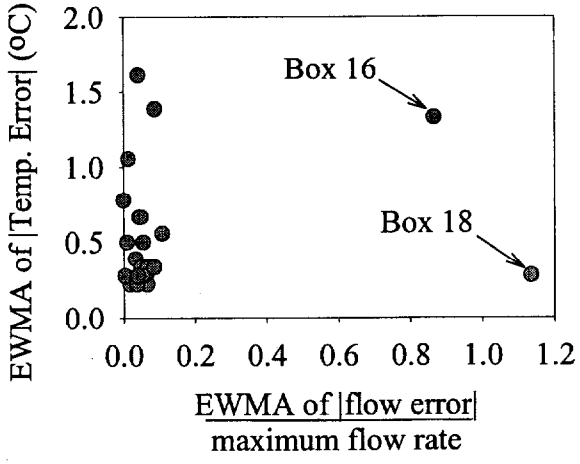

Figure 17d Temperature errors versus normalized flow errors.

REFERENCES

Åström, K. J. and T. Hägglund, *PID Controllers: Theory, Design, and Tuning*, 2nd Edition, Instrument Society of America, Research Triangle Park, North Carolina, 1995.

Box, G. E. P., and G. M. Jenkins, *Time Series Analysis: Forecasting and Control*, Revised-Edition, Holden-Day, San Francisco, 1976.

Hartman, T. B., *Direct Digital Controls for HVAC Systems*, McGraw-Hill, 1993.

Hunter, J. S., "The Exponentially Weighted Moving Average," *Journal of Quality Technology*, Vol. 18, No. 4, pp. 203-209, October 1986.

Lee, W. Y., C. Park, and G. E. Kelly, "Fault Detection of an Air-Handling Unit Using Residual and Recursive Parameter Identification Methods," *ASHRAE Transactions*, Vol. 102 Pt. 1, pp. 528-539, 1996a.

Lee, W. Y., J. M. House, C. Park, and G. E. Kelly, "Fault Diagnosis of an Air-Handling Unit Using Artificial Neural Networks," *ASHRAE Transactions*, Vol. 102 Pt. 1, pp. 540-549, 1996b.

Montgomery, D. C., *Introduction to Statistical Quality Control*, Second Edition, John Wiley & Sons, New York, 1991.

Pandit, S. M, and S. M. Wu, *Time Series and System Analysis with Applications,* John Wiley & Sons, Inc., New York, 1983.

Seborg, D. E., T. F. Edgar, and D. A. Mellichamp, *Process Dynamics and Control*, John Wiley & Sons, New York, 1989.

Wang, S. K., *Handbook of Air Conditioning and Refrigeration*, McGraw-Hill, Inc., New York, 1993.

NOMENCLATURE

Symbols

d	duty cycle of an electric motor
e	process error, $y_{set} - y$
S	number of starts, stops, and reversals of an actuator
T	sampling time of analog-to-digital converter
t	time
t_S	settling time of a controller
u	control signal
Δu	change in control signal
$\underline{X}$	performance index
$\overline{X}$	EWMA of performance index X
y	process output
δ	tolerance limit for process output
λ	exponential smoothing constant

Subscripts

j	time index
set	setpoint value

APPENDIX: PROCEDURE FOR INSTALLING ELECTRIC DAMPER ACTUATOR TO THE VAV BOX

Figure A.1 shows the electric damper and VAV box. The following procedure should be used to attach the motor to the damper:

1. Place the damper blade in the closed position.
2. Slip the coupling for the electric damper actuator over the damper shaft.
3. Attach electric damper actuator to VAV box.
4. Use an Allen wrench to secure the set screw in the coupling to the damper shaft.

When installing the damper actuator for VAV box 18, the damper blade was in the open position instead of the closed position after step 1. This caused the damper blade to be 90 degrees out of position.

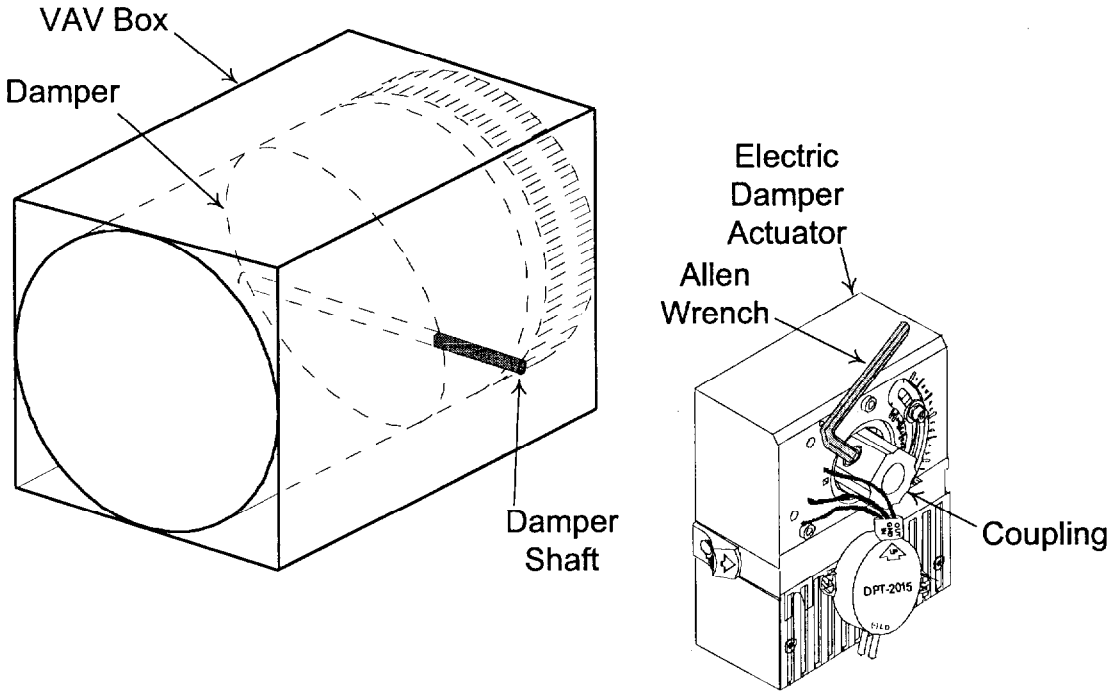

Figure A.1 Damper and electric actuator.